INVESTIGATION OF THE VALIDITY OF MINER'S LAW FOR ASPHALT MIXES

Christiane Weise
Dresden University of Technology, Chair of Pavement Engineering, Dresden, Germany

ABSTRACT

In the 1940ies the linear cumulative damage was hypothesised by Miner on the basis of Uniaxial Tensile Tests on aluminium samples. In Germany Miner's Law is used to determine the fatigue life of asphalt layers in the course of the analytical pavement design process although aluminium and asphalt are different in the known material properties. The purpose of the research project funded by the German Research Foundation (DFG) among other things was to investigate the validity of Miner's Law for asphalt mixes.
Different asphalt mixes have been investigated using the Cyclic Indirect Tensile Test (CITT) with swelling loading. For the determination of fatigue life of asphalt mixes CITT with a constant stress level during the test are conducted. For the investigations of the validity of Miner's Law the results of repeated load tests with constant and variable upper stress levels are compared with each other. For each test with a variable upper stress level the damage sum was determined using Miner's Law. The tests were conducted at five different testing temperatures. So it is possible to describe the coherence between the damage sum and the testing temperature. Furthermore, the influence of the loading frequency on the damage sum was determined considering four different frequencies.
From the test results can be concluded that Miner's Law is dependent on the test temperature, the loading frequency and also on chronological order of the different stresses and strains.

Keywords: Design of pavement, Fatigue Cracking, Indirect tension, Stone Mastic Asphalt

1. PURPOSE OF THE STUDY

Various stresses occur in asphalt pavements as a result of traffic loading and climate impact. Currently, the analytical pavement design process of asphalt pavements is performed regarding the fatigue state at the lower surface of the asphalt base layer and under consideration of the material properties of the used mixes. So it becomes possible to optimize the pavement layers. Within the design process, the damages caused by the numerous load states are added linearly using Miner's Law. Miner's Law has been developed on the basis of uniaxial tensile tests on aluminium samples. That is the reason why the validity of Miner's Law must be verified for asphalt mixes.

2. INTRODUCTION

2.1. Miner's Law

Miner's Law allows the accumulation of different damages. Based on cyclic uniaxial tensile and tensile/compression tests on aluminium samples, Miner introduced the following hypothesis:

$$\sum_i \frac{n_i}{N_i} = 1 \qquad [1]$$

where n_i = number of load cycles applied at stress i
N_i = number of load cycles to failure at stress i

Each load cycle consumes a small quantity of the material's lifetime. According to Miner's Law, the chronological order of the damage does not influence the damage value. In this context, the term endurance limit is used for stresses i where the number of load cycles to failure is infinite, i.e. no damage occurs. The endurance limit could not be verified for asphalts until now. So it must be assumed that the endurance limit does not exist. Furthermore, Miner did not include the endurance limit in his hypothesis.
It has already been proved for other materials, in particular steel that the independence of the damage from the chronological order postulated in Miner's Law does not exist. That means that load cycles with elastic strains below the endurance limit (which exist for steel) causes damage when they occur in combination with load cycles with large elastic strains (Radaj 2007). In other words, the endurance limit depends on the load order.
The tests Miner conducted on aluminium samples already showed large variances of the summation of the different damage portions. The damage sum for the test results published varies between 0.60 and 1.49 (Miner 1945). Miner used the fracture of the sample as damage criterion. Nevertheless, Miner's Law is used in Germany and other countries within the analytical pavement design process.

2.2. Nonlinear damage accumulation

As a rule, nonlinear damage development occurs in technical materials and components. If the damage portion n_i/N_i depends on the stress amplitude, nonlinear damage accumulation becomes the criterion. Equation 2 gives an example of a nonlinear damage process (Radaj 2007).

$$\sum_i \left(\frac{n_i}{N_i} \right)^p = 1 \qquad [2]$$

It must be clarified if this constraint is also valid for asphalt, which means that the damage speed increases with an increasing stress amplitude.
The actual damage that occurs during the test can only be determined using the elastic strain related to the elastic strain at the moment of macro-cracking (fatigue criterion, see section 2.3). Within a test with sinusoidal loading the elastic strain can be calculated using the measured elastic deformation of the specimen in consequence of the sinusoidal loading. If the measured specimen deformation is derived with a sinus function the elastic strain is two times the amplitude.
Figure 1 shows the curves of the weighted elastic strain for three different strain amplitudes caused by three loading amplitudes. The diagram shows that there is no difference in the damage speed. Hence, asphalt has linear damage behaviour.

2.3. Evaluation of fatigue tests

Different fatigue criteria can be used for the evaluation of fatigue tests. For the described tests (cyclic indirect tensile tests, see section 3.1), the method of energy ratio ER based on the concept of dissipated energy (Hopman 1993) has been used to determine the moment of macro-crack formation. The method of energy ratio ER has been used for cyclic indirect tensile tests for the first time by (Read 1996). The fatigue criterion macro-crack formation differs from the common known parameter N_{f50}, which is defined in the European Standard EN 12697-24 and which is insufficient for the investigations described in this paper. For harmonic periodical stresses, the dissipated energy during one load cycle can be calculated using equation 3.

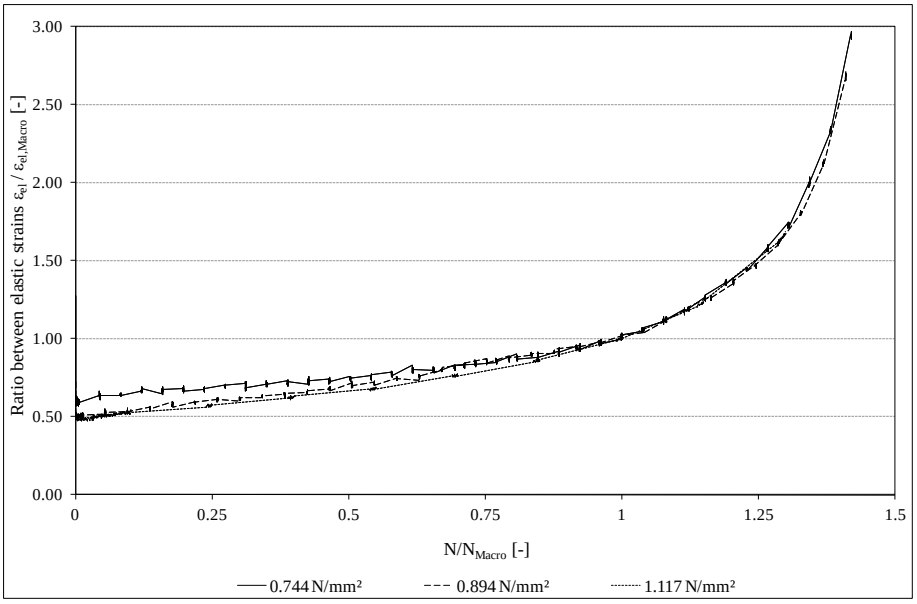

Figure 1: Weighted elastic strain curves $\varepsilon_{el}/\varepsilon_{el,Macro}$ for different loading amplitudes $\Delta\sigma$ for a Stone mastic asphalt SMA 11 S, bitumen 25/55-55A, Gabbro

$$W_i = \pi \cdot \sigma_i \cdot \varepsilon_i \cdot \sin \varphi_i \qquad [3]$$

where W_i = dissipated energy
σ_i = maximum stress
ε_i = elastic strain
φ_i = phase angle between stress and strain

The energy ratio ER relates the dissipated energy of load cycle i to the dissipated energy of the initial state 0 and can be calculated using equation 4.

$$ER(N_i) = \frac{N_i \cdot W_0}{W_i} = \frac{N_i \cdot (\pi \cdot \sigma_0 \cdot \varepsilon_0 \cdot \sin \varphi_0)}{\pi \cdot \sigma_i \cdot \varepsilon_i \cdot \sin \varphi_i} \qquad [4]$$

where N_i = number of load cycles
W = dissipated energy
σ = maximum stress
ε = elastic strain
φ = phase angle between stress and strain

Assuming that during the test the induced stress and also the phase angle are constant ($\sigma_0 = \sigma_i$; φ_I = const.) and $\varepsilon = \sigma/E$, equation 4 can be simplified.

$$ER(N_i) = N_i \cdot E_i \qquad [5]$$

where N_i = number of load cycles
E_i = stiffness modulus

Furthermore, fatigue functions can be arranged on the basis of stress or strain. This research project studies strain-based fatigue functions.

3. LABORATORY TESTS

Cyclic indirect tensile tests (CITTs) are conducted to examine the validity of Miner's Law for asphalt mixes: on the one hand, these were tests with constant stress amplitudes and, on the other, tests with five different loading configurations. The tests and the test conditions are specified in the following sections.
In Germany CITTs are used to conduct the fatigue duration and in addition the mastercurve of the stiffness, which are two necessary input parameters for the pavement design process The real loading of a pavement can be approximated partially by the state of stress within CITT specimen (combination of tension and compression stresses). In contrast to the findings of (Di Benedetto et al. 2004) research projects realized in Germany reveal that the test results of the CITT and for example the 4 Point Bending Test are comparable if the test conditions are similar (Weise et al. 2009). Further-

more, (Di Benedetto et al. 2004) remark, that permanent deformation during the CITT leads to early failure. But permanent deformations occur in all fatigue tests unless they are displacement controlled. The specific nature of the CITT is considered in the German pavement design procedure.

3.1. Cyclic indirect tensile test (CITT)

In CITTs, a circular disk specimen is loaded diametrically between two loading strips (see Figure 2). Because of the specimen shape and the linear transmission of force to the lateral area, an inhomogeneous state of stress occurs in vertical and horizontal directions. FEM calculations verify that the horizontal tensile stress in the middle of the specimen is nearly constant over approximately 70% of the specimen's diameter. In the area of force transfer, horizontal compressive stresses appear. The mean value of the vertical compressive stress is located in the middle of the specimen and the maximum value in the area of load transfer. In the centre of the specimen, the ratio between vertical compressive stress and horizontal tensile stress is 3 to 1.
The dimensions of the samples are chosen as a function of the maximum grain size. For a maximum grain size of 11 mm, the specimen diameter should be 100 mm and the height 40 mm. The loading strips had a width of 12.7 mm (AL Sp - Asphalt 09).

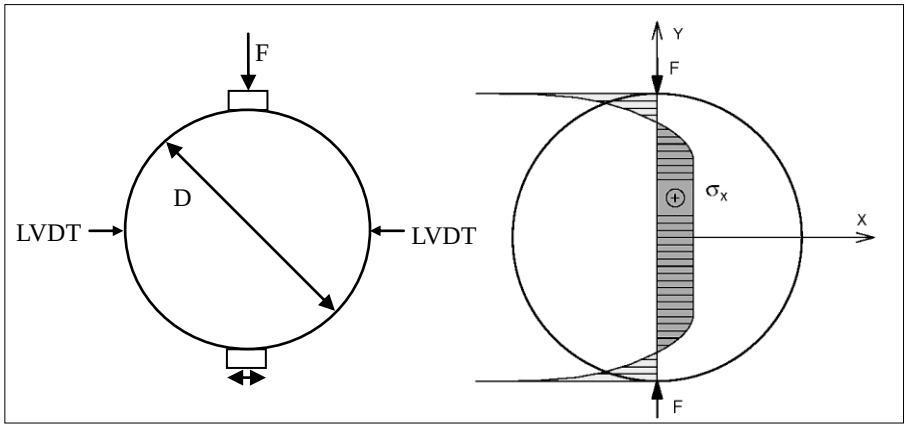

Figure 2: Principle of the CITT and horizontal tensile stress distribution in the middle of the specimen

3.2. Asphalt mixes investigated and sample preparation

Two stone mastic asphalts with a maximum grain size of 11 mm and polymer modified bitumen (SMA 11 S, bitumen 25/55-55A) were used for the tests. On the one SMA 11 S with gabbro and 6.5% polymer modified bitumen for the test regarding load configurations and on the other hand SMA 11 S with moraine and 6.7% polymer modified bitumen for the tests regarding frequency configurations.
The void content of the samples was between 2.69 and 3.77 Vol.-% and 3.0 and 4.23 respectively. This corresponds to a bulk density variance of 0.03 g/cm³. The asphalt mixes were produced in a mixing plant. The asphalt slabs were fabricated in the laboratory using a segmented roller compactor and a deformation-controlled compaction regime. Afterwards, specimens were drilled out of the slabs and the void content as well as the dimensions were determined for each specimen.

3.3. Test conditions for the investigated load configurations

The CITTs have been carried out at 5 Hz. The chosen test temperatures are 10, 2.5, 5, 12.5 and 20 °C. They are evenly spread over the possible temperature range of the CITT. The load, which was applied to the specimen, had the form of a harmonic sinusoidal wave without any rest periods. The wave is defined by lower σ_L and upper stress σ_U. Depending on the test temperature, the cryogenic stress or the necessary contact stress have been chosen as lower stress value. For the determination of fatigue functions, the upper stress has been varied three times. Table 1 gives a summary of the chosen stress values.

Table 1: Test conditions for CITTs

Temperature	Lower stress	Upper stress		
T [°C]	σ_L [N/mm²]	$\sigma_{U;1}$ [N/mm²]	$\sigma_{U;2}$ [N/mm²]	$\sigma_{U;3}$ [N/mm²]
-10	0.845	1.60	1.80	2.20
-2.5	0.312	1.20	1.40	1.70
5	0.106	0.85	1.00	1.223
12.5	0.051	0.50	0.70	0.90
20	0.035*	0.30	0.45	0.60

* necessary contact stress

Fatigue tests with constant stress amplitudes according to AL-SP-Asphalt 09 have been carried out and evaluated and formed the basis for the following tests to verify Miner's Law. Tests with five different load configurations were conducted to prove the validity of Miner's Law. Figure 3 illustrates the chronological order of the different load levels. The duration of each load level depends on the test temperature. The load configurations can be described as:

- configuration A: increasing loading
- configuration B: decreasing loading
- configuration C: alternating loading
- configuration D: cyclic loading

Load configuration D was tested in two versions. In version D50, each loading level has a length of 50 load cycles. In version D500 however, each load level has a duration of 500 load cycles. The lengths of the load levels 1 (low), 2 (medium) and 3 (high) for load configurations A, B and C are given in Table 2.

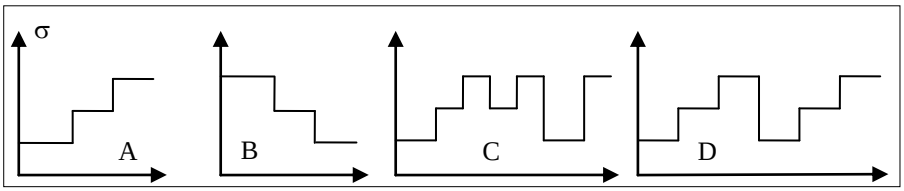

Figure 3: Load configurations

Table 2: Lengths of load levels for load configurations A, B and C depending on the test temperature

T [°C]	load level	load configuration A	load configuration B	load configuration C
-10	1	30,000	60,000	10,000
	2	10,000	10,000	5,000
	3	6,000	2,000	1,000
-2.5	1	15,000	50,000	7,500
	2	6,000	6,000	3,000
	3	5,000	1,000	500
5	1	10,000	30,000	5,000
	2	4,000	2,000	2,000
	3	16,000	1,000	1,000
12.5	1	22,000	50,000	11,000
	2	3,500	3,500	1,750
	3	5,000	1,000	500
20	1	15,000	50,000	5,000
	2	3,000	3,000	2,000
	3	10,000	1,250	1,000

3.4. Test conditions for the investigated frequency configurations

The CITTs have been carried out at 20 °C. The chosen test frequencies are 0.5, 3.125, 5 and 10 Hz. The load, which was applied to the specimen, had the form of a harmonic sinusoidal wave without any rest periods. The wave is defined by lower and upper stress. A necessary contact stress of 0.035 N/mm² has been chosen as lower stress value. For the determination of fatigue functions, the upper stress has been varied three times (1.000, 0.352, 0.273 N/mm²). The frequency configurations have been studied at 0.352 and 0.273 N/mm². Tests with four different frequency configurations were conducted to prove the validity of Miner's Law concerning different loading frequencies. Figure 4 illustrates the chronological order of the different frequency levels. The duration of each load level depends on the upper stress value and is given in Table 3.

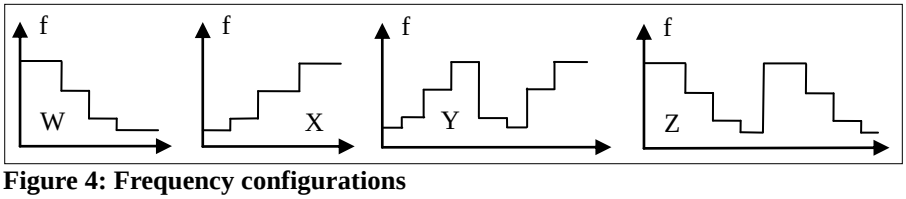

Figure 4: Frequency configurations

Table 3: Lengths of the frequency levels for frequency configurations

Frequency configuration	Frequency [Hz]	σ_U = 0.273 N/mm²	σ_U = 0.352 N/mm²
W	0.5	(15,000)	(6,500)
	3.125	8,000	2,500
	5	12,000	6,000
	10	45,000	10,000
X	0.5	1,250	500
	3.125	8,000	2,500
	5	12,000	6,000
	10	(78,000)	(31,000)
Y	0.5	600	100
	3.125	2,000	1,000
	5	6,000	3,000
	10	20,000	5,000
Z	0.5	250	250
	3.125	250	250
	5	250	250
	10	250	250

3.5. Evaluation of tests
3.5.1. Principle of the Evaluation

Evaluating the fatigue tests with constant stress amplitudes produces strain-based fatigue functions. The fatigue functions are generated for each test temperature to ensure maximum accuracy. Figure 5 shows the five fatigue functions. These results were used to determine the lengths of the different load levels (see Table 2) and the number of load cycles N_i until failure at stresses i.

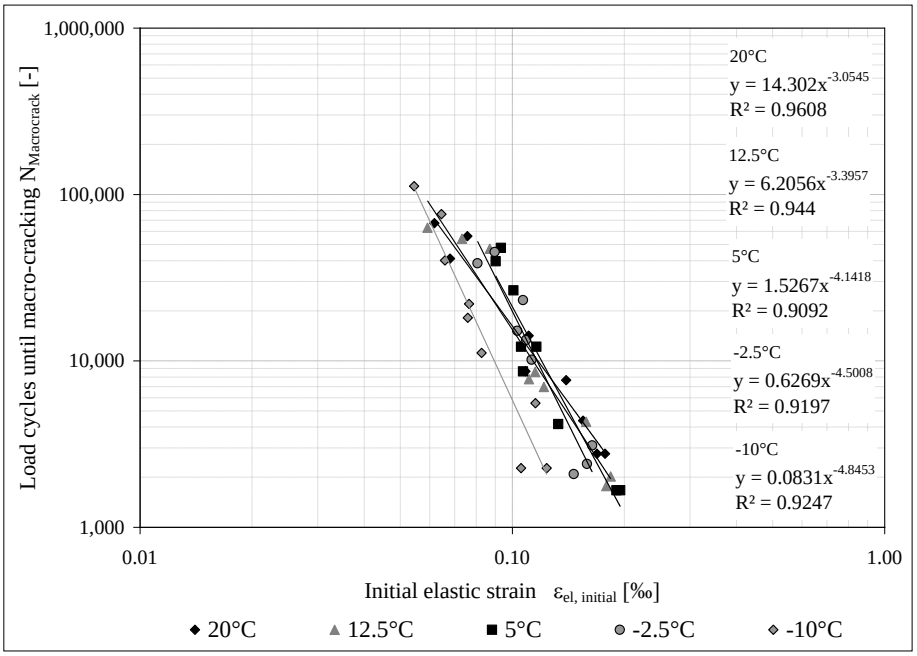

Figure 5: Fatigue functions for the different test temperatures (constant stress amplitudes)

Regular fatigue tests (with constant stress amplitude during the test) conducted at four loading frequencies are the basis for the tests with different frequency configurations. Figure 6 shows the four fatigue functions. Using these results the length of the frequency levels (see Table 3) as well as the number of load cycles until failure N_i could be determined.

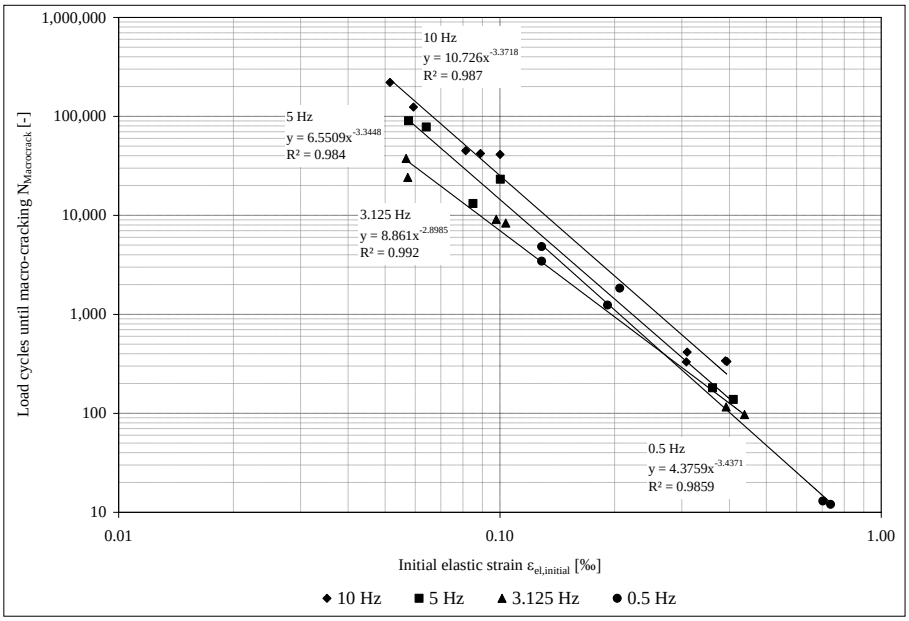

Figure 6: Fatigue functions for the different loading frequencies (constant stress amplitudes)

3.5.2. Evaluation of the investigated load configurations

At the beginning of each test with the varying loading configurations, a pre-test of three times 50 load cycles was performed to determine the initial elastic strain of each load level. Thanks to this procedure, the number of load cycles until failure can be investigated using the fatigue function determined before. Directly after the pre-test, the intended loading configuration was applied to the specimen. Figure 7 illustrates the curve of the energy ratio ER and additionally the dissipated energy of each load cycle for a test conducted at 12.5 °C and loading configuration D500. Points of discontinuity can be observed in the diagram because of the simplified determination of the energy ratio in Equation 5 and the minor impact of the stress amplitude on the stiffness modulus.
The analysis of the tests and the calculation of the damage sum can be conducted according to the following procedure (shown for the example in Figure 7):

- Determination of the initial elastic strain from the pre-test.
  $\varepsilon_{el,1}$ (σ_U=0.5 N/mm²) = 0.085‰
  $\varepsilon_{el,2}$ (σ_U=0.7 N/mm²) = 0.134‰
  $\varepsilon_{el,3}$ (σ_U=0.9 N/mm²) = 0.227‰
- Determination of the number of load cycles until macro-cracking using the curve of the Energy Ratio.
  $N_{Macro\text{-}crack}$ = 5,269
- Comparison of the applied load cycles n_i and the load cycles until failure N_i for each load level using the initial elastic strain.

Level i	n_i	N_i
1	2,000	26,801
2	1,769	5,781
3	1,500	960

- Calculation of the damage sum using Equation 1.

$$\sum_3 \frac{n_i}{N_i} = 0.075 + 0.31 + 1.563 = 1.943$$

3.5.3. Evaluation of the investigated frequency configurations

At the beginning of each test with the varying frequency configurations, a pre-test of altogether 185 load cycles (100 – 50 – 30 – 5) was performed to determine the initial elastic strain of each frequency level. Thanks to this procedure, the number of load cycles until failure can be investigated. Directly after the pre-test, the intended frequency configuration was applied to the specimen. Figure 8 illustrates the curve of the energy ratio ER and the corrected Energy Ratio of each load cycle for a test of frequency configuration W.
Points of discontinuity can be observed in the diagram because of the simplified determination of the energy ratio in Equation 5 and the impact of the loading frequency on the stiffness modulus. Hence, the Energy Ratio was corrected and so it was still possible to determine the moment of macro-crack formation. The difference of the stiffness modulus was calculated when the loading frequency changed. The stiffness modulus of the lower loading frequency was raised about this value. The reference value was the stiffness modulus at 10 Hz. The damage sum was calculated using the procedure described in the previous section.

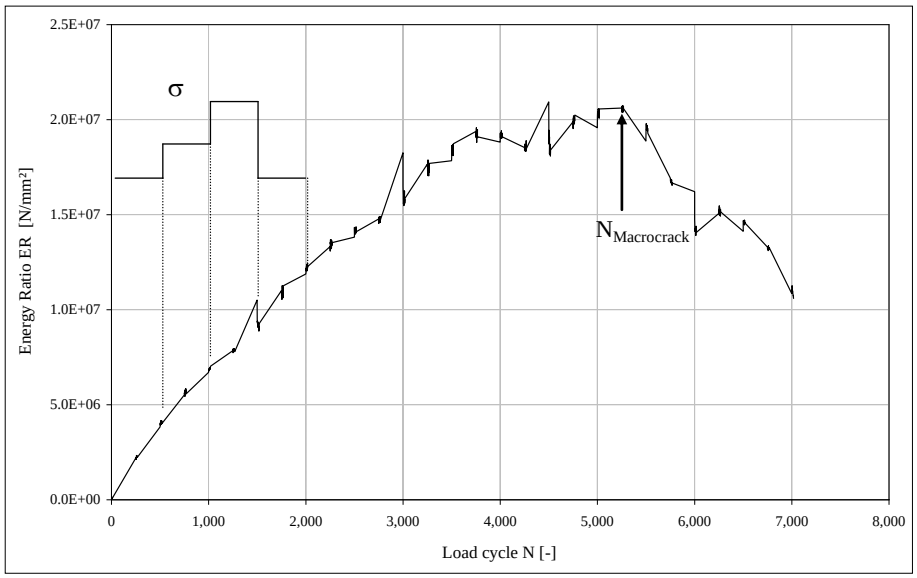

Figure 7: Curve of the Energy Ratio ER (12.5 °C, D500)

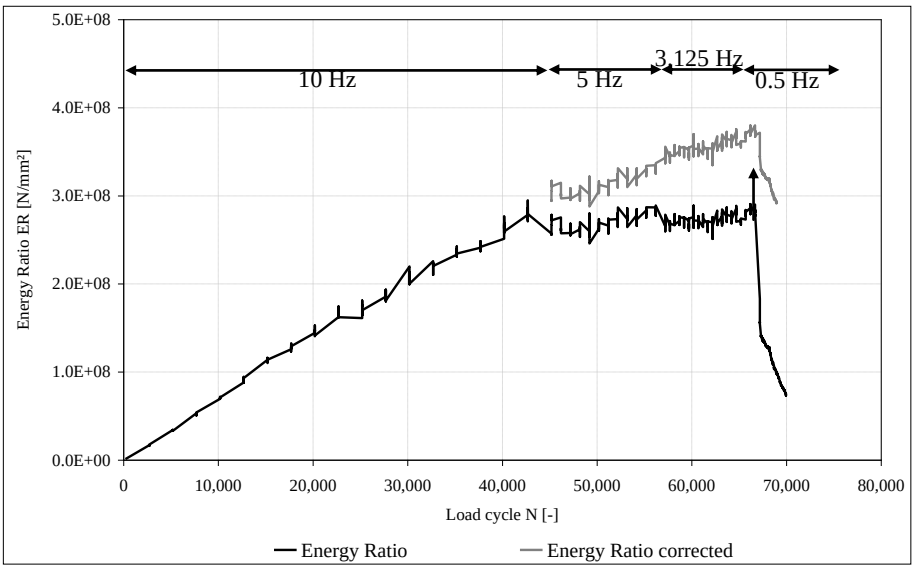

Figure 8: Run of the Energy Ratio ER and the corrected Energy Ratio (Test W)

4. TEST RESULTS

4.1. Impact of the loading sequence

The damage sum of the different loading configurations in Figure 9 shows a clear dependence on the loading configuration and the load order, respectively. The following findings can be derived from the test results:
The damage sum is lower for increasing loading compared with decreasing loading (difference between configuration A and B). That means that a high initial loading does not lead to early failure.
The length of each load level has an important impact on the damage sum. Fast changes in the load level, as it occurs in situ, lead to a lower damage sum (difference between configuration D500 and D50).
It seems to be impossible to derive the dependence of the damage sum from the loading configuration using the test results because random loading configurations occur in situ. Furthermore, recovery, which has a positive effect on the damage sum, cannot be taken into account. Recovery is caused, for example, by rest periods of different lengths. The study of this effect would require real time tests. Furthermore, the scatter of the test results (on the one hand, the number of load cycles until failure and the damage sum, on the other) is really high. It could be observed that the scatter is especially high for low test temperatures and for loading configurations with alternating and cyclic loading. In Figure 9 the range of the damage sum for 5 °C is also given.

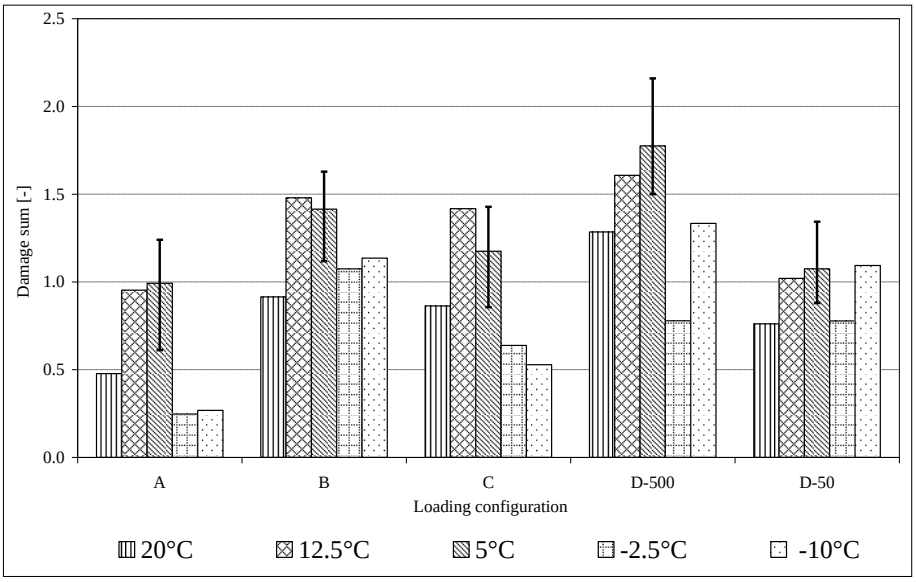

Figure 9: Impact of loading configuration on the damage sum and the range for 5 °C

4.2. Impact of the frequency sequence

In Figure 10 the mean values of the damage sum are given. The results show a clear impact of the frequency sequence on the damage sum. The following findings can be derived from the test results:
(1) The damage sum for decreasing loading frequencies is lower compared to increasing loading frequencies (difference between configuration W and X).
(2) Frequent changes of the loading frequencies (configuration Y) lead to a very small damage sum. However, this form of the frequency configuration is as close as possible on the reality.
A differentiation off the damage sum according to the upper stress value does not seem to be applicable because numerous loading and temperature conditions occur in reality. Hence, only the mean value should be considered.
The range of the damage sum is comparable with the range of the loading configurations. Figure 10 shows also the range of the damage sum fort he upper stress value of 0.352 N/mm².

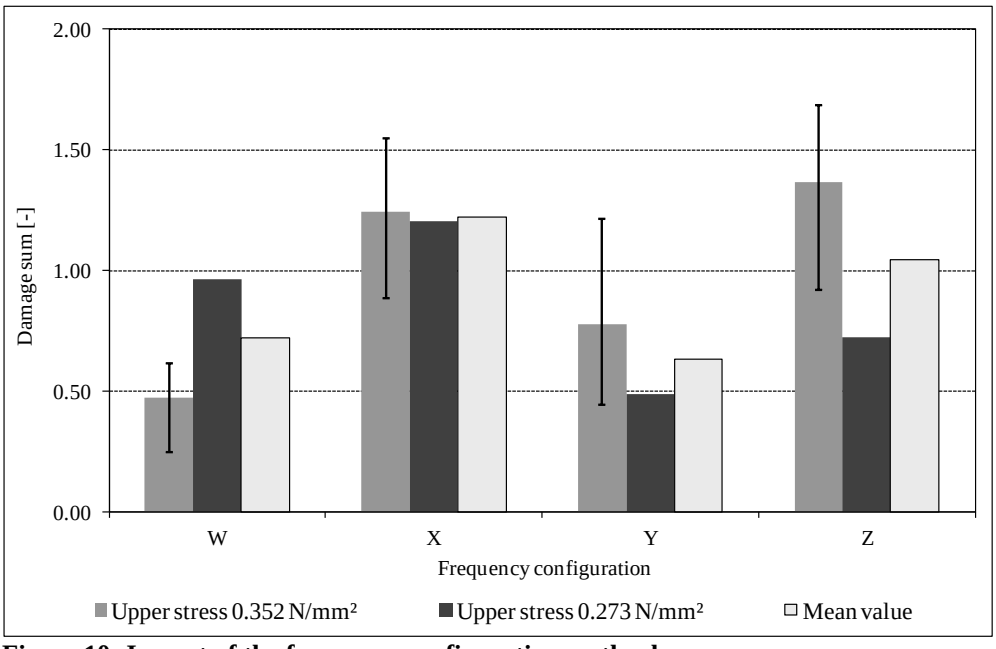

Figure 10: Impact of the frequency configuration on the damage sum

4.3. Reverse loading sequence

In spite of the conclusion that it is not possible to conduct fatigue tests with realistic load configurations further tests concerning the loading sequence were carried out.
Tests at 5 °C (load configuration A and B) have been repeated with the effectively obtained number of load cycles but in reverse order. For several test with load configuration A the macro-crack occurs already at the second load level. That is

the reason why also the reverse tests consist of only two load levels (see Figure 11). The test results are summarised in Table 4.

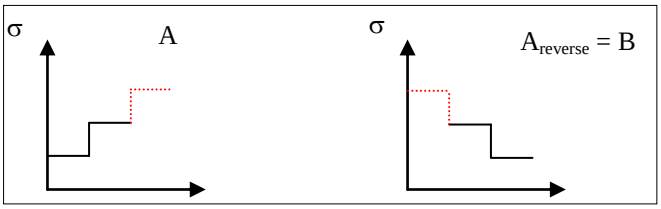

Figure 11: Principle of reverse test using the example of load configuration A

Table 4: Results of the reverse tests

Original Test					Reverse Test				
No.	$N_{\sigma 1}$	$N_{\sigma 2}$	$N_{\sigma 3}$	$\Sigma n_i/N_i$	No.	$N_{\sigma 3}$	$N_{\sigma 2}$	$N_{\sigma 1}$	$\Sigma n_i/N_i$
Loading Configuration A					Loading Configuration $A_{reverse}$ = B				
58-1	10,000	1,619	-*	*0.611*	78-3	-	2,000	30,402	*1.318*
56-1	10,000	2,019	-*	*0.894*	69-4	-	2,000	12,908	*0.555*
56-4	10,000	2,019	-*	*1.223*					
Loading Configuration B					Loading Configuration $B_{reverse}$ = A				
61-3	1,000	2,000	13,519	*1.628*	82-2	20,016	-*	-*	*0.438*
69-3	1,000	2,000	12,019	*1.118*	82-3	12,750	1,615	-*	*0.610*
65-3	1,000	2,000	24,019	*1.497*					

* load level not reached, macro-crack occur earlier

The average value of the damage sum is lower for increasing loading (A) compared to decreasing loading ($A_{reverse}$ = B). This conclusion could be confirmed using the test results with loading configuration A and B (see Figure 9) and the reverse tests as well. The obviously longer life time at decreasing loading can be traced back to recovering effects. In Figure 12 the run of the stiffness modulus for specimen No. 56-1 (configuration A) at the initial phase is given. It is obvious that the stiffness modulus is increasing at decreasing loading (N>150).

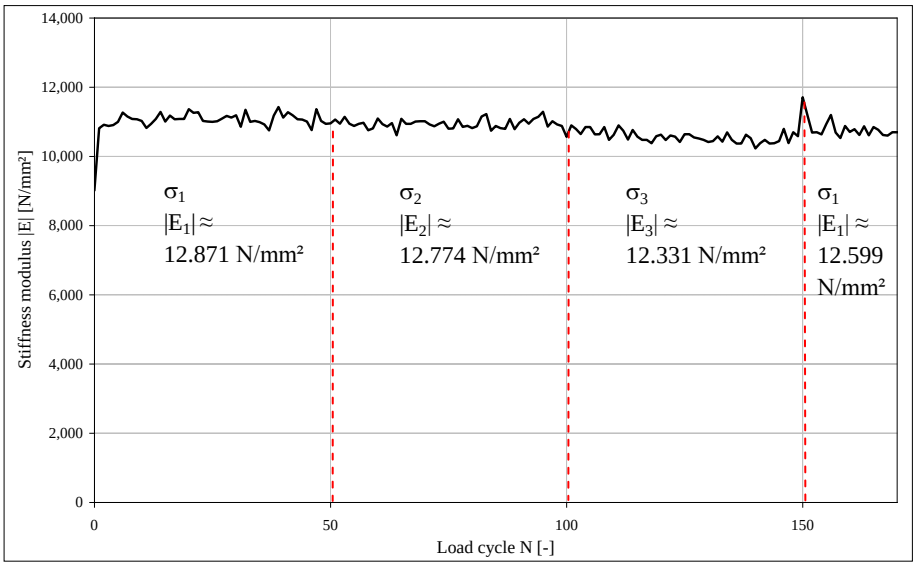

Figure 12: Run of the stiffness modulus |E| during the first 160 load cycles

4.4. Impact of the test temperature

Figure 13 shows the temperature-dependent average values of the damage sum for the five loading configurations. Without considering the loading configuration, the average value of the damage sum is nonlinear over the test temperature. The minimum and maximum values caused by different loading configurations are also given in Figure 13. The average value of the damage sum is larger than 1.0 for test temperatures 5 and 12.5 °C. For the other temperatures, the values are below 1.0. If you calculate the average over the given values again, you obtain 1.002 which is the failure criterion postulated by Miner. This approach assumes that Miner's Law is valid for asphalt mixes under the given conditions.

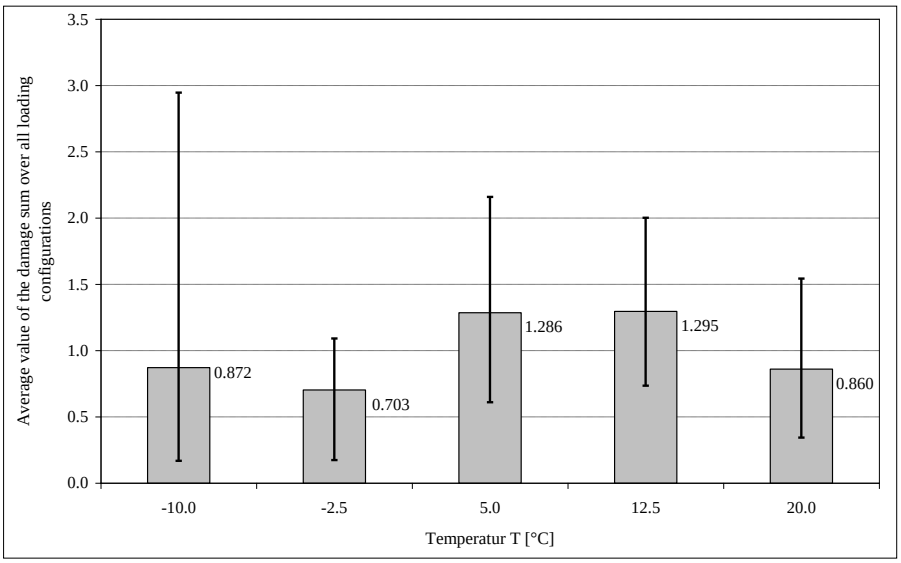

Figure 13: Impact of test temperature on damage sum (average over all load configurations)

It must be taken into account that temperatures within an asphalt pavement did not appear at the same frequency. Figure 14 gives the temperature distribution of the surface temperature for Zone 5 (Kayser 2007) in Germany including e.g. Dresden. The temperature levels are divided into 5 K intervals and characterised by the mean value. The first step was to calculate the frequencies of the temperature levels -10, 5 and 20 °C using the characteristic values of the two neighbouring values. Because the sum of the frequencies of the five test temperatures is not 100% the frequencies have to be reweighted. By linking the determined temperature frequencies h(T) with the damage sum $n_i/N_i(T)$ and adding all single terms we obtain different damage sums for the six temperature zones defined for Germany (see Table 5). These results indicate that the used temperature distributions obviously lead to a compensation of the high and low parts of the damage sum.

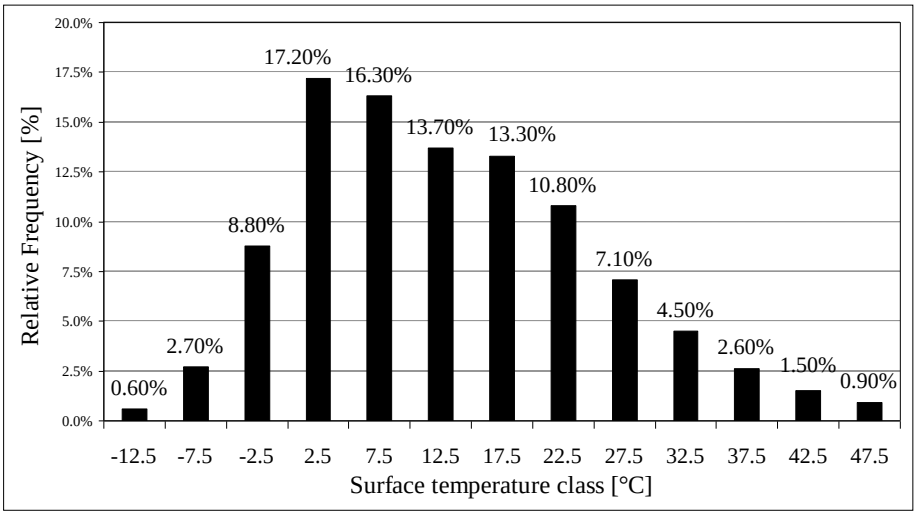

Figure 14: Frequency distribution of the surface temperature for Zone 5 (Kayser 2007)

Table 5: Damage sums for the temperature zones defined for Germany

Temperature Zone	Temperature weighted damage sum
1	1.092
2	1.070
3	1.075
4	1.086
5	1.082
Mountains	1.036

This result indicates that the used temperature distributions obviously lead to a compensation of the high and low parts of the damage sum. In order to confirm this result, more temperature distributions must be investigated.

5. CONCLUSION

The investigation of five different loading configurations at five test temperatures shows a clear impact of the load order and the test temperature on the damage sum at failure.
The impact of the test temperature is of particular importance because the real loading order cannot be taken into account especially with regard to the impact of rest periods. It is not possible to determine this effect using accelerated tests. The damage sum obtained on the basis of the test results in combination with a real temperature distribution is 1.08. Considering the test results of the CITTs and the test conditions (especially the temperature), the validity of a hypothesis of linear damage accumulation can be confirmed.
The CITT and also other fatigue tests can be conducted at a maximum test temperature of 20 °C only. Hence, the impact of higher temperatures on the damage sum cannot be investigated for now.
The tests concerning different frequency configurations reveal that the damage sum is influenced by the configuration of the loading frequencies which represents the vehicle speed. Currently it does not seem to be possible to integrate the test results in the analytical pavement design process. Further research and models concerning the loading frequency e.g. in different depths of the asphalt pavement or in dependence of the material stiffness are necessary.
The test results published by Miner already showed a large scatter which can be confirmed by the current test results. From this it follows that the use of statistic methods is required. In the future, it will be possible to consider different security levels by using cumulative frequency curves.

ACKNOWLEDGEMENT

The author gratefully acknowledges the financial support of the DFG – German Research Foundation (Deutsche Forschungsgemeinschaft, DFG 1642/5-1), the assistance of Prof. Dr.-Ing. habil. Frohmut Wellner and all colleagues at the Chair of Pavement Engineering, TU Dresden.

REFERENCES

AL Sp - Asphalt 09, Test methods for the design of asphalt pavements: Method for the determination of the stiffness and fatigue characteristics of bituminous mixes using the indirect tensile test (in German), Forschungsgesellschaft für Straßen- und Verkehrswesen, FGSV-Verlag, Köln, Germany, 2009.

Di Benedetto, H.; de La Roche, C.; Baaj, H.; Pronk, A. & Lundström, R., "Fatigue of bituminous mixtures", Materials and Structures, Vol. 37, pp. 202-216, 2004.

EN 12697-24, Bituminous mixtures – Test methods for hot mix asphalt – Part 24:Resistance to fatigue, 2004.

Radaj, D.; Vormwald, M., „Fatigue Strength" (Ermüdungsfestigkeit - Grundlagen für Ingenieure), Springer-Verlag, Berlin, Germany, 2007.

Read, J., "Fatigue cracking of bituminous paving mixtures", University of Nottingham, Department of Civil Engineering, PhD thesis, Nottingham, Great Britain, 1996.

Kayser, S., „Principles for survey of climatic influences within the flexible pavement design process" (Grundlagen zur Erfassung klimatischer Einflüsse für Dimensionierungsrechnungen von Asphaltbefestigungen), PhD thesis, Dresden University of Technology, Germany, 2007.

Miner, M. A., "Cumulative damage in fatigue", Journal of Applied Mechanics, Vol. 12, Issue 3, pp. 158-165, 1945.

Hopman, P.; Kunst, P. & Pronk, A., "A Renewed Interpretation Model for Fatigue Measurement. Verification of Miner's Rule", 4th Eurobitume Symposium, Vol. 1, p. 557-561, Madrid, Spain, 4-6 October 1989.

Weise, C.; Werkmeister, S.; Wellner, F. & Oeser, M., "Determination of the Fatigue Behaviour of asphalt base mixes using the indirect tensile and the 4 point bending Test", 2nd Workshop on 4PB, University of Minho, Guimaraes, Portugal, 24-25th September 2009.